Julio A. Deiber[1]
María V. Piaggio[2]
Marta B. Peirotti[1]

[1]Instituto de Desarrollo Tecnológico para la Industria Química (INTEC), Universidad Nacional del Litoral (UNL), Consejo Nacional de Investigaciones Científicas y Técnicas (CONICET), Santa Fe, Argentina
[2]Cátedra de Bioquímica Básica de Macromoléculas, Facultad de Bioquímica y Ciencias Biológicas, UNL, Santa Fe, Argentina

Received August 21, 2012
Revised October 3, 2012
Accepted October 17, 2012

Research Article

Determination of electrokinetic and hydrodynamic parameters of proteins by modeling their electrophoretic mobilities through the electrically charged spherical soft particle

This work explores the possibility of using the electrically charged "spherical soft particle" (SSP) to model the electrophoretic mobility of proteins in the low charge regime. The general framework concerning the electrophoretic mobility of the SSP already presented in the literature is analyzed and discussed here in particular for polyampholyte-polypeptide chains. In this regard, this theory is applied to BSA for different protocol pH values. The physicochemical conditions required to model proteins as SSP from their experimentally determined electrophoretic mobilities are established. In particular, the protein charge regulation phenomenon and the SSP particle core are included to study BSA having isoelectric point p$I \approx 5.71$, within a wide range of bulk pH values. The results of this case study are compared with previous ones concerning the spherical porous particle and the spherical hard particle with occluded water. A discussion of chain conformations in the SSP polyampholyte layer is presented through estimations of the packing and friction fractal dimensions.

Keywords:
Polyampholyte spherical soft particle / Polypeptide permeability / Protein electrophoretic mobility / Protein friction fractal dimension / Protein packing fractal dimension
DOI 10.1002/elps.201200463

Additional supporting information may be found in the online version of this article at the publisher's web-site

1 Introduction

At present, relevant conclusions on the conformation, size, electrical state, and hydration of polypeptides have been achieved through physicochemical models of their electrophoretic mobility μ_p as described, for instance, in [1–35] and many citations therein. These models have been benefited by modern CZE experimental techniques, which are well discussed in [36–38] and citations therein. Also, there is a high number of experimental polypeptide electrophoretic mobility μ_p^{exp} data in the low charge regime available for their study and interpretation within this modeling framework (see [14, 18] and the Supporting Information for details on the meaning of the low charge regime). For these purposes, the type of particle used in CZE models is important. Typically one can apply, for instance, electrophoretic mobility expressions proposed for a near aspherical hard particle (AHP) with occluded BGE solvent [12–18] and the spherical soft particle (SSP) composed by a particle core and a polyampholyte layer where BGE solvent flows [39–49]. The SSP can represent asymptotically two relevant particular cases; one is the spherical hard particle (SHP) [50] while the other is the spherical porous particle (SPP) (Hermans–Fujita model, [51]). The AHP, SHP, and SPP were already applied to model electrophoretic mobility of proteins as described for instance in [1–8, 12–14, 17, 18, 52]. Part of these studies was based on the framework of the

Correspondence: Dr. Julio A. Deiber, Instituto de Desarrollo Tecnológico para la Industria Química (INTEC), Universidad Nacional del Litoral (UNL), Consejo Nacional de Investigaciones Científicas y Técnicas (CONICET), Güemes 3450, S3000GLN, Santa Fe, Argentina
E-mail: treoflu@santafe-conicet.gov.ar
Fax: +54-(0)342-4550944

Abbreviations: AAS, amino acid sequence; **AHP**, aspherical hard particle; **HCF**, hydrated chain fractal; **PLLCEM**, perturbed Linderstrøm-Lang capillary electrophoresis model; **SHP**, spherical hard particle; **SPP**, spherical porous particle; **SSP**, spherical soft particle

perturbed Linderstrøm–Lang capillary electrophoresis model (PLLCEM) mainly by considering approximate expressions to quantify the charge regulation phenomenon in proteins [12, 14, 17]. One of the purposes was to show that globular proteins satisfied their functions in a pH different from the bulk pH where they were immersed. Thus there exists a regulated average <pH> in the protein domain depending on both its charge state and interaction with the BGE. In general it was shown that the charge regulation phenomenon pushes <pH> values toward protein isoelectric point p*I*, indicating that the so-called "bulk pH" regularly used to evaluate the protein charge state requires further quantitative considerations. Certainly these results may have a relevant impact on protein functions in biological systems, for instance concerning optimal enzymatic performance and protein–ligand interactions.

In this analysis it is also interesting to point out that the types of particles described above, provide as main information the solvent-particle friction f (force on particle divided its translation velocity) to be assigned to the polypeptide chain and also the possibility to study chain conformations by using the simple hydrated chain fractal (HCF) model [14–18] where the expression $f = 6\pi\eta_s a_o N^{g_f}$ applies. Here, g_f is the friction fractal dimension and η_s is the solvent viscosity. Also, the size of each amino acid residue is associated with a radius a_o evaluated as the arithmetic average radius of van der Waals radii of N amino acid residues in the amino acid sequence (AAS) with molar mass M. Thus the HCF is composed of a solvent domain where the polypeptide chain is immersed. This solvent domain is structurally a part of the protein, where water molecules and ions may have a residing time along the translation of the whole particle. It is then clear that for these purposes polypeptides are modeled as a chain of N beads (in this regard important details are provided in [9–11]). Therefore two random fractals like those defined in [14–18, 52] may be useful to characterize the polypeptide chain from the hydrodynamic and electrokinetic points of views once the solvent–particle friction f and effective charge number Z have been estimated. One is the chain packing fractal with dimension g_p describing the spatial ($g_p \to 3$) to linear ($g_p \to 1$) distribution of polypeptide amino acid residues in the associated solvent. The other is the chain friction fractal indicating when the polypeptide chain is mainly in the collapsed, hybrid and polyelectrolyte regimes by estimating the value of the friction fractal dimension g_f within the range $1/3 < g_f < 1$. This fractal dimension must be analyzed for $1/3 < g_f < 3/5$ (from the collapsed state to the onset of important hydrodynamic interaction around the Flory theta condition at $g_f \approx 1/2$) and for $3/5 < g_f < 1$ when effective solvent flow through the SPP occurs (see details in [52]). The former range was mostly found through the friction of AHP where the shape is the controlling physical aspect, while the later one belonged to the SPP as described in [52]. Here, we will show that the SSP applied to proteins also yields $g_f > 3/5$ as discussed below, by placing emphasis on the occurrence of BGE solvent flow through the particle.

The purpose of this work is specifically to extend our study in [52] to the SSP, where apart from the polyampholyte domain present in the SPP a particle core may be also found. Here once more the BGE solution is characterized through values of pH, ionic strength I, η_s, electrical permittivity ε, temperature T and Debye–Hückel parameter $\kappa = \sqrt{2e^2 \mathrm{I} N_A 10^3/(\varepsilon k_B T)}$, while the moving particle has assigned a Stokes hydrodynamic radius a_H as a measure of the protein domain including hydration. Throughout this work Avogadro and Boltzmann constants are designated N_A and k_B, respectively, while e is the elementary charge. It is also assumed that the protein low charge regime is achieved. Thus a linear relationship between electrophoretic mobility and surface potential may be approximately established. In this regime ion polarization-relaxation due to the flowing BGE around the electrically driven particle may be neglected [17, 18]. For a discussion on this aspect see for instance [4, 53]. It must be observed here that the zeta potential $\zeta = eZ/\{4\pi\varepsilon a_H(1 + \kappa a_H)\}$ of SHP obtained from the solution of the linearized Poisson–Boltzmann equations does not apply to the SSP.

In this work, the polypeptide effective charge number is evaluated through $Z = \sum_i Z_i n_i$ [12, 13, 52], where Z_i and n_i are the charge number and the number of each i-ionizing group of amino acid residues in the polypeptide chain, respectively, including $-NH_2$ and –COOH terminal groups (see further details in [17, 52] and citations therein).

By considering the above theoretical outline, this work explores the possibility of using electrically charged SSP to model the electrophoretic mobility of polyampholyte-polypeptide. In this regard, the general expressions of μ_p involving the SSP provided and widely analyzed by Ohshima [39–44] are used and applied here, specifically to proteins in conjunction with theoretical aspects concerning the charge regulation phenomenon already described in [12–14, 17, 18] and more recently in [52] for the SPP. Since we keep working in the low charge regime, once more ion polarization relaxation of the BGE is neglected in the present framework.

This work is organized as follows. In Section 2, theoretical aspects involving the electrophoretic mobility modeling of the general electrically charged SSP [39–44] are described and complemented theoretically to be able to consider polyampholyte-polypeptide chains. In Section 3, the discussion of results is presented indicating the conditions under which a polyampholyte-polypeptide electrophoretic mobility may be modeled through a charged SSP. The globular protein used to illustrate the model proposed here is the BSA. The experimental electrophoretic mobility data of this protein was reported in [54] for different protocol pH values (see also Table 1 and [52]). Although the temperature value was not explicitly reported in [54], calculations of thermophysical properties indicate a temperature close to 25°C. In Section 3 a critical analysis of results is carried out and concluding remarks are provided in Section 4.

Table 1. Numerical estimations of BSA electrokinetic and hydrodynamic properties through the SSP model as a function of bulk pH at 25°C

pH	3	4	7	8	9	10	11
$\mu_p \times 10^8 (\frac{m^2}{Vs})$	2.77	1.50	−1.73	−2.25	−2.68	−3.03	−3.18
b(Å)	79.75	80.96	35.24	38.84	38.79	43.58	61.31
δ	18.57	19.46	0.96	1.52	1.51	2.44	8.05
H_d	67 430	70 580	2180	4258	4236	7670	28 427
H	68 479	71 761	3524	5598	5570	8985	29 685
<pH>	3.67	4.36	6.55	7.40	8.28	9.18	10.14
<ψ>(mV)	39.43	21.17	−26.64	−35.43	−42.26	−48.72	−50.53
Z	77.64	43.14	−10.49	−16.42	−19.54	−27.67	−55.96
Z_w	93.96	62.50	−14.35	−18.47	−25.06	−50.31	−87.48
$\rho_{fix} \times 10^{-7}$ (C/m^3)	0.59	0.32	−1.12	−1.24	−1.48	−1.41	−0.96
τ	0.98	0.98	0.77	0.84	0.84	0.89	0.96
$K \times 10^{19}$ (m^2)	16.01	16.61	4.19	4.54	4.54	5.15	8.97
g_p	1.76	1.75	2.40	2.29	2.29	2.18	1.91
g_f	0.94	0.94	0.72	0.76	0.76	0.81	0.90
$\lambda \times 10^{-9}$(m^{-2})	0.79	0.78	1.55	1.48	1.48	1.39	1.06

For the meaning of all symbols presented, please see the text, where they are first defined, or the total list of symbols in the Supporting Information.
The following constants are used: $a = 20$ Å, $N = 583$, $v_p = 0.71$ cm^3/g, $M = 66\,387$ g/mol, $a_o = 2.92$ Å, $a_c = 26.51$ Å, p$I = 5.71$, and I ≈ 10 mM, $M_d = 37\,896$ g/mol, $M_d/M = 0.571$, $N_d = 333$. The protein permeability K is calculated through Eq. (15).

2 Modeling

By following closer the developments and nomenclature in [39–42] and additional details provided in [52], it is clear that the SSP is composed of an uncharged particle core of radius a covered by a polyampholyte layer of thickness $d = b - a$, where b is the radius of the whole particle. Therefore a characteristic magnitude is the friction density γ evaluating the resistance offered to the flow of BGE solution by chain segments distributed in the polyampholyte layer of thickness d. It is also convenient to define parameter $\lambda = (\gamma/\eta_s)^{1/2}$ [39,40], and the constant fixed charge density $\rho_{fix} = 3eZ/[4\pi(b^3 - a^3)]$ uniformly distributed throughout the polyampholyte layer as simpler case (see also [46, 47, 55] for more general considerations). The polypeptide mass must be distributed between the particle core and the polyampholyte layer requiring $a < a_c$ where $a_c = \{3Mv_p/(4\pi N_A)\}^{1/3}$ is the protein compact radius defined in [14] and v_p is the average specific volume of the polypeptide AAS as described in [52]. These expressions also imply that the chain molar mass $M_d = 4\pi(a_c^3 - a^3)N_A/(3v_p)$ located in the polyampholyte layer is the fraction $M_d/M < 1$ of the total polypeptide molar mass M. Therefore one can estimate that the number of amino acid residues residing on the average in the polyampholyte layer is $N_d \approx M_d/M_m$, where M_m is the arithmetic average molar mass of amino acid residues in the AAS. Further, the ionizing and polar amino acid residues are the most probably ones present in the polyampholyte layer accounting the number N_d; hence, this value depends on the AAS of the polypeptide under study. It is then clear that as a first approximation $a \approx a_o(N - N_d)^{1/3}$, as obtained through a simple balance of chain beads. The hydrophilic amino acid residues composing on the average N_d are Asn, Asp, Arg, Cys, Gln, Glu, His, Lys, Ser, Thr, and Tyr. The constraint $a < a_c$ in the SSP is also useful to analyze protein hydration $\delta \approx \{(b/a_c)^3 - 1\}v_p/v_w$ (expressed as mass of water per mass of protein) and physical aspects associated with the existence of a particle core in the SSP composed on the average of hydrophobic amino acid residues like Ala, Ile, Leu, Met, Phe, Pro, Trp, and Val. Also Gly is assumed amphiphilic and it can be distributed between the particle core and polyampholyte layer. Although they may still have associated some hydration on physical grounds as discussed in [14, 56–59] despite of their hydrophobic nature, here we assume that for the protein states around the native one, the hydrations of these amino acid residues have been squeezed out during the folding process. This physical aspect is consistent with the hypothesis stated in [39–42] indicating that electrolyte-free ions cannot penetrate the particle core. Thus, in principle, the particle core is assumed rather anhydrous to keep working rigorously in the SSP model framework.

After the above considerations involving the SSP core, we can redefine the fractal-packing dimension associated with the polyampholyte layer (see [52] for the SPP) as follows:

$$g_p = \log(N_d)/\log\left\{(b^3 - a^3)^{1/3}/a_o\right\} \quad (1)$$

The electrophoretic mobility expressions of the general charged SSP in the low charge regime involves several hypotheses stated in [39–42]. Additional theoretical considerations are also introduced in [52], to allow in principle the application of this particle model to polyampholyte-polypeptide chains [17, 18]. Thus, two general analytic expressions for the electrophoretic mobility of a charged SSP were provided by Ohshima in [39–42] as discussed in [52]. Both models yield the same asymptotic expressions as reported in [41] although

the later one is preferred and used here as follows:

$$\mu_p = \frac{b^2}{9}\int_b^\infty \left[3\left(1-\frac{r^2}{b^2}\right)-\frac{2L_2}{L_1}\left(1-\frac{r^3}{b^3}\right)\right]G(r)\,dr + \frac{2L_3}{3\lambda^2 L_1}\int_a^\infty\left(1+\frac{r^3}{2b^3}\right)G(r)dr - \frac{2}{3\lambda^2}\int_a^b\left[1-\frac{3a}{2\lambda^2 b^3 L_1}\left\{(L_3+L_4\lambda r)\ \cosh[\lambda(r-a)] - (L_4+L_3\lambda r)\ \sinh[\lambda(r-a)]\right\}\right]G(r)dr \quad (2)$$

where, the following equations of $G(r)$ applies for the low charge regime:

$$G(r) = \frac{\rho_{fix}}{\eta_s}\left(1+\frac{a^3}{2r^3}\right)\left(\frac{1+\kappa b}{1+\kappa a}\right)\exp(-\kappa(b-a)) \times\left\{\frac{\kappa^2 r\cosh(\kappa(r-a))-\kappa\ \sinh(\kappa(r-a))}{(\kappa r)^2} + \frac{a\kappa r\ \sinh(\kappa(r-a))-a\cosh(\kappa(r-a))}{r^2}\right\} \quad (3)$$

when $a < r < b$, and:

$$G(r)=\frac{\varepsilon\kappa^2\psi_o b}{\eta_s}\left(1+\frac{a^3}{2r^3}\right)\left(\frac{1+\kappa r}{r^2}\right)\exp(-\kappa(r-(b))) \quad (4)$$

for $r > b$. In addition:

$$\psi_o = \frac{\rho_{fix}}{2\varepsilon\kappa^2} \times\left\{1-\frac{1}{\kappa b}+\frac{(1-\kappa a)(1+\kappa b)}{(1+\kappa a)\kappa b}\exp[-2\kappa(b-a)]\right\} \quad (5)$$

is the surface electrical potential at $r = b$. Parameters L_1, L_2, L_3, and L_4 are functions of a, b, and λ as follows:

$$L_1 = \left(1+\frac{a^3}{2b^3}+\frac{3a}{2\lambda^2 b^3}-\frac{3a^2}{2\lambda^2 b^4}\right)\cosh[\lambda(b-a)] -\left(1-\frac{3a^2}{2b^2}+\frac{a^3}{2b^3}+\frac{3a}{2\lambda^2 b^3}\right)\frac{\sinh[\lambda(b-a)]}{\lambda b} \quad (6)$$

$$L_2 = \left(1+\frac{a^3}{2b^3}+\frac{3a}{2\lambda^2 b^3}\right)\cosh[\lambda(b-a)] +\frac{3a^2}{2b^2}\frac{\sinh[\lambda(b-a)]}{\lambda b}-\frac{3a}{2\lambda^2 b^3} \quad (7)$$

$$L_3 = \cosh[\lambda(b-a)]-\frac{\sinh[\lambda(b-a)]}{\lambda b}-\frac{a}{b} \quad (8)$$

$$L_4 = \sinh[\lambda(b-a)]-\frac{\cosh[\lambda(b-a)]}{\lambda b}+\frac{\lambda a^2}{3b}+\frac{2\lambda b^2}{3a} +\frac{1}{\lambda b} \quad (9)$$

Further, the asymptotic response of this model for $\lambda \to \infty$, indicates that the electrophoretic mobility of a charged SSP with no flow of the BGE solution through the polyampholyte layer of thickness d is obtained. Nevertheless emphasis must be placed on the fact that the diffusion fluxes of BGE free ions in and out of this layer are still allowed. For this reason, when $\lambda \to \infty$ one refers to the "spherical semisoft particle" model [42]. For this situation, the following expression applies [40, 41]:

$$\mu_p = \frac{b^2}{9}\int_b^\infty\left(1-\frac{3r^2}{b^2}+\frac{2r^3}{b^3}\right)G(r)dr \quad (10)$$

When the particle core radius tends to the particle radius ($a \to b$) the SHP is obtained and Eq. (10) is again applicable, but the function $G(r)$ is different from that of the case $\lambda \to \infty$ (see Eqs. (3–5)). Further, when the particle core is null ($a = 0$) the analytical expression for the SPP electrophoretic mobility is obtained [40, 42, 51]. This last result has been already applied to proteins in [52] by including the charge regulation phenomenon.

A crucial parameter in the SSP model is ρ_{fix} involving the polypeptide effective charge number Z, which is different from the wild charge number Z_w obtained from numerical titration [12]. Since weak i-ionizing groups in the polyampholyte layer are partially dissociated and their charge numbers Z_i are quantified from reference pK_i^r and average regulating <pH> giving ΔpK_i-shift values [12], the charge regulation phenomenon around protein ionizing groups allows one the estimation of <pH> as follows [12, 52]:

$$<pH> = pH + \frac{e<\psi>}{\ln(10)\ k_B T} \quad (11)$$

where $<\psi>$ is the average value of the equilibrium particle electrical potential evaluated in the polyampholyte layer through:

$$<\psi> = \frac{3}{(b^3-a^3)}\int_a^b \psi^{(o)}(r)r^2 dr \quad (12)$$

The equilibrium electrical potential $\psi^{(o)}(r)$ for $a < r < b$ and $r > b$ is reported in [42].

Following [52] in relation to protein hydration, the total number of water molecules per polypeptide chain $H = \delta M/18$ is equal to the water captured by the amino acid residues placed in the polyampholyte layer plus the number of water molecules H_d due to the degree of protein denaturation. These values depend on protocol pH and consequently on <pH> as demonstrated below. Thus the following expression may be used as a first approximation to this complex phenomenon [58] where the hydration of non polar amino acid residues are eliminated because they are assumed to be

forming the particle core:

$$\begin{aligned} H &= h^I_{t\text{-COOH}}\,|Z_{\text{COOH}}| + h^I_{t\text{-NH}_3^+}\left|Z_{\text{NH}_3^+}\right| \\ &\quad + h^{\text{PI}}_{t\text{-COOH}}(1-|Z_{\text{COOH}}|) + h^{\text{PI}}_{t\text{-NH}_3^+}(1-Z_{\text{NH}_3^+}) \\ &\quad + \sum_i^N \left\{h^I_i\,|Z_i| + h^{\text{PI}}_i(1-|Z_i|) + h^P_i\right\} + H_d \\ &= M((b/a_c)^3-1)v_p/(18v_w) \end{aligned} \tag{13}$$

Here, h^I_i and h^{PI}_i are the numbers of water molecules of ionizing and polar-ionizing i-amino acid residues, weighed through their charge number $Z_i = \pm 1/(1+10^{\mp(pK^r_i - <\text{pH}>)})$ as a consequence of their dual electrostatic character, while h^P_i stands for the number of water molecules of polar i-amino acids residues. In Eq. (13), $h^I_{t\text{-COOH}}$, $h^I_{t\text{-NH}_3^+}$, $h^{\text{PI}}_{t\text{-COOH}}$, and $h^{\text{PI}}_{t\text{-NH}_3^+}$ are the corresponding values for ionizing and polar-ionizing terminal groups (see [13, 58] for further details on the estimation of the numbers of water molecules and reference pK_i designated pK^r_i). Also the effective protein charge number is $Z = \sum_i n_i Z_i$, where the summation is carried out for each type of ionizing groups in the AAS. Equation (13) is different from that reported in [52] because hydrations h^{NP}_i of nonionizing and non polar i-amino acid residues have been excluded taking into account that hydrophobic amino acid residues are assumed on the average anhydrous as indicated above. Also in this regard, around a half of the amphiphilic Gly number is included in the sum of Eq. (13) as a first approximation (see also below).

Following [52] the closure of Eq. (2) for the SSP electrophoretic mobility requires the estimation of parameter $\lambda \approx 1/K^{1/2}$. Therefore models of the average permeability K available in the literature are used (see [52, 55] and citations therein). For instance, the so-called dilute model provides:

$$K \approx 2a_o^2/(9\tau_p) \tag{14}$$

where $\tau_p \approx N_d a_o^3/(b^3-a^3)$ is the polypeptide volume fraction in the hydrated SSP polyampholyte domain, and $\tau \approx 1-\tau_p$ is the corresponding porosity. When hydrodynamic interaction between pairs of amino acid residues is important, the following permeability expression applies [60–62]:

$$K = \frac{2a_o^2}{9\tau_p}\left(1 + \frac{3}{\sqrt{2}}\tau_p^{1/2} + \frac{135}{64}\tau_p \ln\tau_p + 16.45\tau_p + \cdots\right) \tag{15}$$

where leading terms of the sum are considered [62]. From previous definitions in [14, 15, 17, 52] one also finds that K is related to the packing and friction fractal dimensions through $\tau_p \approx a_o^{(3-g_p)}/\{b^3-a^3\}^{(1-g_p/3)}$ and $g_f = \log\{2(b^3-a^3)/9a_oK\}/\log(N_d)$, respectively. Thus, asymptotically $g_f = 1$ for the free draining dilute model (Eq. (14)). It is also clear that Eqs. (14) and (15) for the SSP are quite different from their counterparts of the SPP used in [52], because here the particle core has been accounted in the definition of τ_p.

Equations (1) to (15) were used in a numerical code to fit experimental data of BSA electrophoretic mobility at different pH values. The procedure is quite simple; thus, for $a \approx a_o(N-N_d)^{1/3}$, trial values of b and H_d are iterated until Eq. (13) is satisfied and the calculated mobility μ_p (Eq. (2)) converges to the experimental mobility μ_p^{exp} within an acceptable relative error less than 10^{-3}. The Supporting Information presents a brief description of this numerical code. Once the problem has been solved, complementary parameters and properties are evaluated.

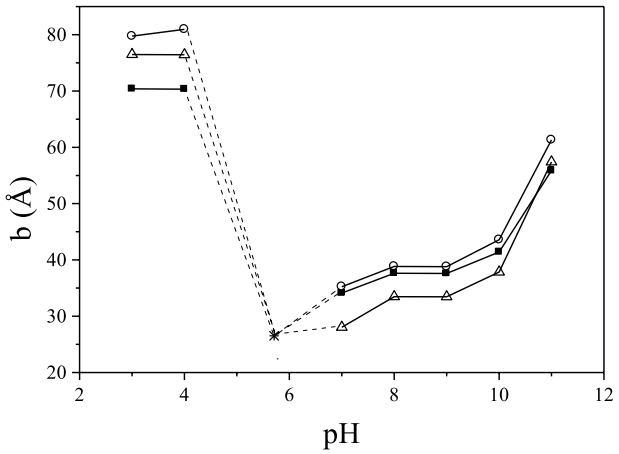

Figure 1. BSA radius b as a function of bulk pH. Symbols are: (○) SSP (Table 1), (■) SPP (Supporting Information Table SI-3), and (Δ) SHP (Supporting Information Table SI-4). Dash and full lines are placed to indicate numerical trends only. Symbol (*) indicates the ideal isoelectric point defined for $a = b \to a_c$, $\delta \to 0$, $g_p \to 3$, and $g_f \to 1/3$. The numerical p*I* estimated is 5.71.

3 Results and discussion

From the analysis of the AAS of BSA and by considering the distribution of amino acid residues described above in relation to the particle core and polyampholyte layer of the SSP, it is found that a good estimate on the average for this protein is $a \approx a_o(N-N_d)^{1/3} \approx 20$ Å. For this specific situation, Table 1 presents values of $\rho_{\text{fix}} = 3eZ/\{4\pi(b^3-a^3)\}$ obtained through the numerical algorithm involving the SSP model. Table 1 also shows numerical predictions of the SSP model for the most relevant electrokinetic and hydrodynamic properties. As pointed out previously in [52] where the SPP with $a = 0$ was used for the BSA protein, here once more parameters and properties emerging from the SSP showed a significant dependence on bulk pH as expected. In general we found that the SSP model predictions of b, δ, ρ_{fix}, $<\text{pH}>$, $<\psi>$, Z, g_p, g_f, λ, K, and τ (see nomenclature in the Supporting Information) followed the same physicochemical trends with variations of pH as those already reported in [52]. Nevertheless quantitative differences are observed, for instance, in Figs. 1–3 and Supporting Information Fig. SI-1. In fact, numerical values obtained from these models show higher differences as the radius of the particle core is increased from $a \approx 0$ to 20 Å yielding finally the SHP for $a = b$ (Tables 1 and Supporting Information Tables SI-1 to SI-4). This last case is also obtained from the PLLCEM when a SHP is considered and small perturbation due to electrostatic

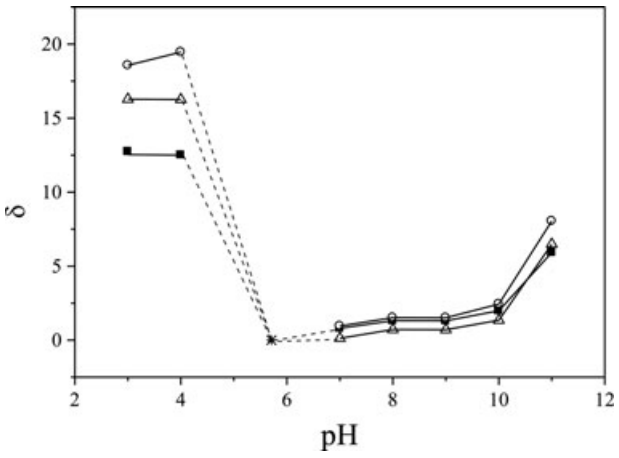

Figure 2. BSA hydration δ as a function of bulk pH. Symbols are: (○) SSP (Table 1), (■) SPP (Supporting Information Table SI-3), and (Δ) SHP (Supporting Information Table SI-4). Dash and full lines are placed to indicate numerical trends only. Symbol (*) indicates the ideal isoelectric point defined for $a = b \to a_c$, $\delta \to 0$, $g_p \to 3$, and $g_f \to 1/3$. The numerical p*I* estimated is 5.71.

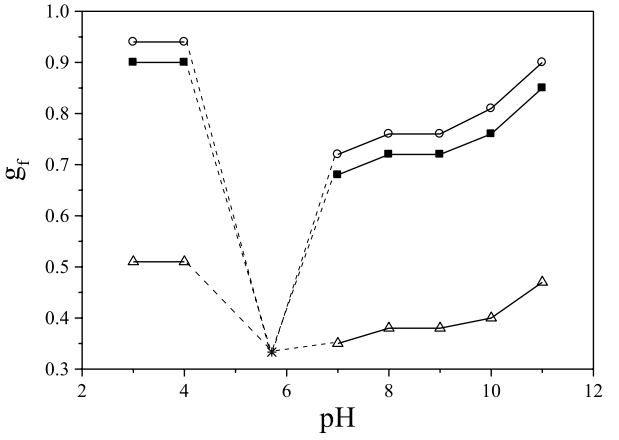

Figure 3. BSA friction fractal dimension g_f as a function of bulk pH. Symbols are: (○) SSP (Table 1), (■) SPP (Supporting InformationTable SI-3) and (Δ) SHP (Supporting Information Table SI-4). Dash and full lines are placed to indicate numerical trends only. Symbol (*) indicates the ideal isoelectric point defined for $a = b \to a_c$, $\delta \to 0$, $g_p \to 3$, and $g_f \to 1/3$. The numerical p*I* estimated is 5.71.

interaction are neglected, as it was already done in Eq. (11) and in [52] to keep consistency with the hypotheses introduced in the models used here (see also physical considerations in [12]). Therefore, when the size of the particle core is rather small, results approach consistently those predicted by the SPP as one expects from the theoretical framework of both models. For lower particle core values than that expected ($a \approx 20$ Å and $N_d = 333$) from the hydrophilic-hydrophobic balance provided by the AAS, one is assuming in addition that some hydrophobic amino acid groups may be out of the protein core by adding their structural hydrations h_i^{NP}. For instance, increasing values of $N_d = 477$, 552, and 583 can be used as indicated in Supporting Information Tables SI-1 to SI-3 for $a \approx 15$, 10, and 0 Å, respectively. Consequently, for these particular cases, the hydration redistribution balance between h_i^{NP} and H_d terms must be considered in Eq. (13).

Another physical aspect to be pointed out here is that the ranges of values taken by parameters λ, K, τ, g_f, and g_p, provide as a first approximation information concerning the conformational states of protein strands placed in the polyampholyte layer only. In fact the "anhydrous" protein molar mass ($M - M_d$) of the particle core is in the collapsed state. In this regard, one observes from Table 1 that the polyampholyte layer presents similar conformational states than those already found when the SPP is used (see Tables 1 and Supporting Information Table SI-3; the last one is reproduced from [52]). In fact the range $3/5 < g_f < 1$ is again found indicating that as far as the polyampholyte layer includes BGE flow, the hydrodynamic interaction between pairs of amino acid residues is relevant and the friction fractal dimension tends toward the range where the free draining situation is an extreme. Further, interesting is the fact that the SSP allows the presence of a collapsed zone with $g_f = 1/3$ (particle core) coexisting with the layer zone, which may present flow through protein strands with significant hydrodynamic interaction between amino acid residues. On the other hand, the SHP yields lower values of friction fractal dimension mainly within $1/3 < g_f < 3/5$ (Fig. 3) around the Flory theta condition as stated in Section 1.

In addition, we found numerically that the asymptotic Eq. (10) does not apply to predict μ_p^{exp} of BSA for the case of the semisoft spherical particle when the pH takes values around the BSA native states (fitting for pH 7 was not found); in fact, this equation gives too low numerical μ_p requiring also rather low hydration values. On the other hand, when $a \to b$, Eq. (10) provides the same results as those obtained for the SHP via PLLCEM as it must be expected proving also the consistency of the calculations carried out within the SSP framework.

From a wider point of view, it is clear that the modeling of the experimental electrophoretic mobility of polypeptides through different types of particles like SSP, SPP, AHP, and SHP allows one to estimate the solvent-chain friction as the main property, which in turn may be interpreted through the HCF as a means to find important properties concerning protein characterizations at different pH values. Thus, at this level of electrically charged chain scales, it is possible to visualize the interplay among hydration, characteristic sizes, and electrostatic states associated with the polypeptide chain fractal dimensions. Finally, it is interesting to visualize in Supporting Information Fig. SI-4 that the BSA packing fractal dimension evaluated from these particles at different pH values decreases for the protein denature states; thus more open and linear chain conformations are obtained as expected, by taking into account that the ideal protein isoelectric point has $g_p \approx 3$.

Before ending this section, it is crucial to visualize that the experimentally measured mobilities of proteins are necessary for the determination of their electrokinetic and hydrodynamic parameters. Therefore in the framework of the

experimental CZE technique, it is required to place emphasis in that mobilities have to be reported at well-defined values of pH, ionic strength, and temperature of BGEs.

4 Concluding remarks

The electrophoretic mobility expression of the electrically charged SSP in the low charged regime is shown to be useful to physically interpret experimental electrophoretic mobility of proteins. As far as flow of the BGE solution through the particle is allowed, the friction fractal dimension takes values within the range 3/5 to 1, quite above from the collapse globule regime. Thus one expects that models involving the SSP described here and the SPP presented previously may be applied well mainly for denatured states of globular proteins and for those native proteins in rather open conformations, where hydrations may be relatively high.

Finally, it is relevant to point out that the experimentally measured mobilities of proteins at well-defined pH, ionic strength and temperature are necessary for the determination of their electrokinetic and hydrodynamic parameters.

Authors wish to thank the financial aid received from Universidad Nacional del Litoral, Santa Fe, Argentina (CAI+D 2009) and CONICET (PIP 112–200801-01106).

The authors have declared no conflict of interest.

5 References

[1] Allison, S. A., *Macromolecules* 1996, *29*, 7391–7401.

[2] Allison, S. A., Potter, M., McCammon, J. A., *Biophys. J.* 1997, *73*, 133–140.

[3] Allison, S. A., *Macromolecules* 1998, *31*, 4464–4474.

[4] Allison, S. A., *Biophys. Chem.* 2001, *93*, 197–213.

[5] Allison, S., Wall, S., Rasmusson, M., *J. Colloid Interface Sci.* 2003, *263*, 84–98.

[6] Allison, S. A., Carbeck, J. D., Chen, C., Burkes, F., *J. Phys. Chem. B* 2004, *108*, 4516–4524.

[7] Allison, S. A., *J. Colloid Interface Sci.* 2005, *282*, 231–237.

[8] Allison, S. A., Pei, H., Allen, M., Brown, J., Chang-II, K., Zhen, Y., *J. Sep. Sci.* 2010, *33*, 2439–2446.

[9] Xin, Y., Mitchell, H., Cameron, H., Allison, S. A., *J. Phys. Chem. B* 2006, *110*, 1038–1045.

[10] Pei, H., Xin, Y., Allison, S. A., *J. Sep. Sci.* 2008, *31*, 555–564.

[11] Pei, H., Allison, S., *J. Chromatogr. A.* 2009, *1216*, 1908–1916.

[12] Piaggio, M. V., Peirotti, M. B., Deiber, J. A., *Electrophoresis* 2005, *26*, 3232–3246.

[13] Piaggio, M. V., Peirotti, M. B., Deiber, J. A., *Electrophoresis* 2007, *28*, 2223–2234.

[14] Piaggio, M. V., Peirotti, M. B., Deiber, J. A., *Electrophoresis* 2009, *30*, 2328–2336.

[15] Piaggio, M. V., Peirotti, M. B., Deiber, J. A., *J. Sep. Sci.* 2010, *33*, 2423–2429.

[16] Peirotti, M. B., Piaggio, M. V., Deiber, J. A., *J. Sep. Sci.* 2008, *31*, 548–554.

[17] Deiber, J. A., Piaggio, M. V., Peirotti, M. B., *Electrophoresis* 2011, *32*, 2779–2787.

[18] Deiber, J. A., Piaggio, M. V., Peirotti, M. B., *Electrophoresis* 2012, *33*, 990–999.

[19] Sharma, U., Negin, R. S., Carbeck, J. D., *J. Phys. Chem. B* 2003, *107*, 4653–4666.

[20] Adamson, N. J., Reynolds, E. C., *J. Chromatogr. B* 1997, *699*, 133–147.

[21] Gitlin, I., Mayer, M., Whitesides, G. M., *J. Phys. Chem. B* 2003, *107*, 1466–1472.

[22] Messana, I., Rossetti, D. V., Cassiano, L., Misiti, F., Giardina, B., Castagnola, M., *J. Chromatogr. B* 1997, *699*, 149–171.

[23] Castagnola, M., Rossetti, D. V., Cassiano, L., Misiti, F., Pennacchietti, L., Giardina, B., Messana, I., *Electrophoresis* 1996, *17*, 1925–1930.

[24] Castagnola, M., Rossetti, D. V., Corda, M., Pellegrini, M., Misiti, F., Olianas, A., Giardina, B., Messana, I., *Electrophoresis* 1998, *19*, 2273–2277.

[25] Adamson, N. J., Reynolds, E. C., *J. Chromatogr. B* 1997, *699*, 133–147.

[26] Cifuentes, A., Poppe, H., *Electrophoresis* 1997, *18*, 2362–2376.

[27] Šolínová, V., Kašička, V., Koval, D., Hlaváček, J., *Electrophoresis* 2004, *25*, 2299–2308.

[28] Benavente, F., Balaguer, E., Barbosa, J., Sanz-Nebot, V., *J. Chromatogr. A* 2006, *1117*, 94–102.

[29] Šolínová, V., Kašička, V., Sázelová, P., Barth, T., Mikšík, I., *J. Chromatogr. A* 2007, *1155*, 146–153.

[30] García de la Torre, J., Huertas, M. L., Carrasco, B., *Biophys. J.* 2000, *78*, 719–730.

[31] García de la Torre, J., *Biophys. Chem.* 2001, *93*, 159–170.

[32] García de la Torre, J., Amorós, D., Ortega, A., *Eur. Biophys. J.* 2010, *39*, 381–388.

[33] Amorós, D., Ortega, A., Harding, S. E., García de la Torre, J., *Eur. Biophys. J.* 2010, *39*, 361–370.

[34] Aragon, S. R., Hahn, D. K., *Biophys. J.* 2006, *91*, 1591–1603.

[35] Aragon, S. R., *Methods* 2011, *54*, 101–114.

[36] Dolník, V., *Electrophoresis* 2008, *29*, 143–156.

[37] El Rassi, Z., *Electrophoresis* 2010, *31*, 174–191.

[38] Kasicka, V., *Electrophoresis* 2012, *33*, 48–73.

[39] Ohshima, H., *J. Colloid Interface Sci.* 1994, *163*, 474–483.

[40] Ohshima, H., *Adv. Colloid Interface Sci.* 1995, *62*, 189–235.

[41] Ohshima, H., *J. Colloid Interface Sci.* 2000, *228*, 190–193.

[42] Ohshima, H., *Electrophoresis* 2006, *27*, 526–533.

[43] Ohshima, H., *Colloid Polym. Sci.* 2007, *285*, 1411–1421.

[44] Ohshima, H., *Sci. Technol. Adv. Mater.* 2009, 063001.

[45] Ohshima, H., *Colloids Surf. A: Physicochem. Eng. Aspects* 2011, *376*, 72–75.

[46] Duval, J. F. L., Ohshima, H., *Langmuir* 2006, *22*, 3533–3546.

[47] Chou, C.-H., Hsu, J.-P., Kuo, C.-C., Ohshima, H., Tseng, S., Wu, R. M., *Colloids Surf. B: Biointerfaces* 2012, *93*, 154–160.

[48] Hill, R. J., Saville, D. A., Russel, W. B., *J. Colloid Interface Sci.* 2003, *258*, 56–74.

[49] Hill, R. J., Saville, D. A., *Colloids Surf. A* 2005, *267*, 31–49.

[50] Henry, D. C., *Proc. R. Soc. London, Ser. A* 1931, *133*, 106–129.

[51] Hermans, J. J., Fujita, H., *Koninkl. Ned. Akad. Wetenschap. Proc. Ser. B* 1955, *58*, 182–187.

[52] Deiber, J. A., Piaggio, M. V., Peirotti, M. B., *Electrophoresis* 2013, *34*, 700–707.

[53] O´Brien, R. W., White, L. R., *J. Chem. Soc. Faraday Trans.* 1978, *74*, 1607–1626.

[54] Menon, M. K., Zydney, A. L., *Anal. Chem.* 1998, *70*, 1581–1584.

[55] Veerapaneni, S., Wiesner, M. R., *J. Colloid Interface Sci.* 1996, *177*, 45–57.

[56] Kuntz, I. D., *J. Am.Chem. Soc.* 1971, *93*, 514–516.

[57] Kuntz, I. D., *J. Am.Chem. Soc.* 1971, *93*, 516–518.

[58] Piaggio, M. V., Peirotti, M. B., Deiber, J. A., *Electrophoresis* 2007, *28*, 3658–3673.

[59] Fennema, O., in: Whitaker, J. R., Tannenbaum, S. R. (Eds.), *Food Proteins*, AVI Publishing, Connecticut 1977, pp. 50–90.

[60] Howells, I. D., *J. Fluid Mechanics* 1974, *64*, 449–475.

[61] Hinch, E. J., *J. Fluid Mechanics* 1977, *83*, 695–720.

[62] Kim, S., Russel, W. B., *J. Fluid Mechanics* 1985, *154*, 269–286.

